Fluorescent Probes | Hot Paper

How to cite:
International Edition: doi.org/10.1002/anie.202114594
German Edition: doi.org/10.1002/ange.202114594

An Activity-Based Ratiometric Fluorescent Probe for In Vivo Real-Time Imaging of Hydrogen Molecules

Wanjun Gong, Lingdong Jiang, Yanxia Zhu, Mengna Jiang, Danyang Chen, Zhaokui Jin, Shucun Qin, Zhiqiang Yu, and Qianjun He**

Abstract: *To reveal the biomedical effects and mechanisms of hydrogen molecules urgently needs hydrogen molecular imaging probes as an imperative tool, but the development of these probes is extremely challenging. A catalytic hydrogenation strategy is proposed to design and synthesize a ratiometric fluorescent probe by encapsulating Pd nanoparticles and conjugating azido-/coumarin-modified fluorophore into mesoporous silica nanoparticles, realizing in vitro and in vivo fluorescence imaging of hydrogen molecules. The developed hydrogen probe exhibits high sensitivity, rapid responsivity, high selectivity and low detection limit, enabling rapid and real-time detection of hydrogen molecules both in cells and in the body of animal and plant. By application of the developed fluorescent probe, we have directly observed the super-high transmembrane and ultrafast transport abilities of hydrogen molecules in cells, animals and plants, and discovered in vivo high diffusion of hydrogen molecules.*

Introduction

Molecular hydrogen is both a clean and green energy source and a well-proven biosafe and effective medical gas, demonstrating a NO-similar wide-spectrum therapeutic effect in a variety of oxidative stress (OS)-related diseases such as ischemic tissue injury, cardiovascular disease, metabolic syndrome, cancer and so on,[1–8] owing to its selective anti-oxidation ability.[2] In addition, molecular hydrogen also is a green and efficient agricultural gas that has significant anti-OS biological effects in enhancement of various tolerances (drug, drought, heavy metals, and salt stress), increase crop yields and freshness preservation.[9–13] Compared with other gas molecules (NO, CO, H_2S, etc.) with biological and medical effects, hydrogen molecules have the smallest molecular weight, the lowest polarity, and the strongest tissue penetration ability, and can therefore rapidly transfer in the body of plants and animals where it has biological effects.[14,15] This feature endows hydrogen molecules with potential advantages for overcoming biological barriers such as the blood–brain barrier (BBB) that cannot be crossed by general drugs. But their pharmacokinetic behaviors, especially behaviors across biological barriers, have not been directly and effectively elucidated, mainly owing to no suitable detection method.

In vivo detection of hydrogen molecules is vitally important to understand their biological effects, in vivo transport and targeting behaviors, as well as the relationship between their dose and therapeutic efficacy. Several approaches and types of equipment for detecting hydrogen molecules in the body have been developed, including isotope tagging, gas chromatography (GC), and hydrogen electrode.[14,15] But detected tissues have to be extracted and homogenized for isotope and GC measurements, losing temporal and spatial resolutions. The hydrogen electrode method is applicable to in vivo monitoring hydrogen concentration in real time, but only one point can be measured, leading to limited spatial resolution. By comparison, molecular imaging probes can be utilized to trace detected molecules in vivo in real time with higher temporal and spatial flexibility, lower tissue damage, higher stability (less external interference), higher specificity, and higher sensitivity. Therefore, the development of hydrogen molecular probes for in vivo and in vitro hydrogen detection is of great significance to understand its biological behaviors and mechanisms, but is extremely challenging because high chemical inertness, high diffusibility and low solubility (1.6 ppm) of hydrogen molecules necessitates extra-high sensitivity of the hydrogen molecular probe.

Recently, a new branch of the chemical sensor field has attracted attention. Different from the traditional detection methods based on lock-and-key binding, the activity-based sensing (ABS) strategy takes advantages of chemical reactivity to design probes.[16–18] Based on the ABS strategy, we designed and synthesized a ratiometric fluorescent hydrogen probe by encapsulating Pd nanoparticles and conjugating azido-/coumarin-modified fluorophore into PEG-modified mesoporous silica nanoparticles (NDI-N_3/Pd@MSN-PEG). Based on a noble metal catalytic hydrogenation strategy, a large amount of small-sized Pd nanoparticles encapsulated

[*] Dr. W. Gong, Dr. D. Chen, Prof. Q. He
Center of Hydrogen Science, Shanghai Jiao Tong University
Shanghai 200240 (China)
E-mail: nanoflower@126.com

Dr. W. Gong, Prof. Z. Yu
School of Pharmaceutical Sciences, Southern Medical University
Guangzhou 510515, Guangdong (China)
E-mail: yuzq@smu.edu.cn

Dr. L. Jiang, Y. Zhu, M. Jiang, Dr. D. Chen, Z. Jin, Prof. Q. He
Marshall Laboratory of Biomedical Engineering, School of Biomedical Engineering, Health Science Center, Shenzhen University
No. 1066 Xueyuan Avenue, Shenzhen 518060, Guangdong (China)

Prof. S. Qin, Prof. Q. He
Institute of Atherosclerosis, Taishan Institute for Hydrogen Biological Medicine, Shandong First Medical University & Shandong Academy of Medical Sciences
Tai'an 271000, Shandong (China)

in MSN were employed to rapidly capture hydrogen molecules and then in situ catalyze them into highly active hydrogen atoms for hydrogenation of NDI-N_3 into NDI-NH_2, enabling fluorescence emission around 540 nm (Figure 1). In addition, coumarin as a fluorescence reference was also conjugated onto NDI-N_3 to construct a ratiometric probe for enhanced detection accuracy. The developed hydrogen probe exhibited high selectivity, rapid responsivity, high sensitivity, and a low detection limit (26.7 nM). The probe was used to successfully detect hydrogen molecules in vitro and in vivo and verify the super-high transmembrane ability of hydrogen molecules in animals and plants. The proposed catalytic hydrogenation strategy will open a bright window for engineering advanced hydrogen probes, and the developed fluorescent hydrogen probe in this work can become a universal tool to aid the study of hydrogen biology and medicine.

Results and Discussion

Probe design

It is difficult for hydrogen molecules to quickly react with general fluorescent dyes under physiological conditions owing to the high energy barrier of the chemical reaction. In order to overcome the energy barrier, we propose a catalytic strategy for designing hydrogen molecular probes. It is well known that catalysis mediated by noble metals such as Pd, Pt, In, etc. can make it easier for hydrogen gas to reduce unsaturated carbon–carbon bonds, nitrogen oxides and carbon oxides at room temperature and under atmospheric pressure.[19–22] Furthermore, nitrogen-containing functional groups are often able to influence the photophysical properties of their neighboring fluorophores, such as blue/red-shifting of the maximum emission wavelength and changes in the molar extinction coefficient, fluorescence quantum yield and fluorescence lifetime. We recognized that azide can be reduced into amine by some reductants[23–25] or catalytic hydrogenation, and that azide and amine have totally opposite electron-absorbing/donating behaviors, causing fluorescence quenching and enhancement of adjacent fluorophores by azide and amine modifications, respectively. Therefore, we have constructed hydrogen molecular probes by conjugating a Pd catalyst with an azide-modified naphthalimide as a fluorophore.

Firstly, we attempted to synthesize a small-molecule hydrogen probe (NDI′-N_3-TPY-Pd) by using a Pd coordination compound as the catalyst (as illustrated in the Supporting Information, Route (1) in Figure S1). However, the probe showed a low sensitivity for hydrogen detection, as it took as long as 10 min of H_2 gas bubbling to achieve a two-fold increase of fluorescence intensity (Figure S1a). Even though the catalytic segment TPY-Pd was detached from the detection segment NDI′-N_3 (as illustrated by Route (2) in Figure S1), the detection efficiency had not been improved distinctly (Figure S1b), indicating that the catalytic activity of the Pd coordination compound TPY-Pd was insufficient for quick hydrogen detection. By comparison, the catalytic hydrogenation efficiency of Pd nanoparticles was much higher (Figure S1b). Pd nanoparticles quickly catalyzed the hydrogenation of NDI″-N_3 with a

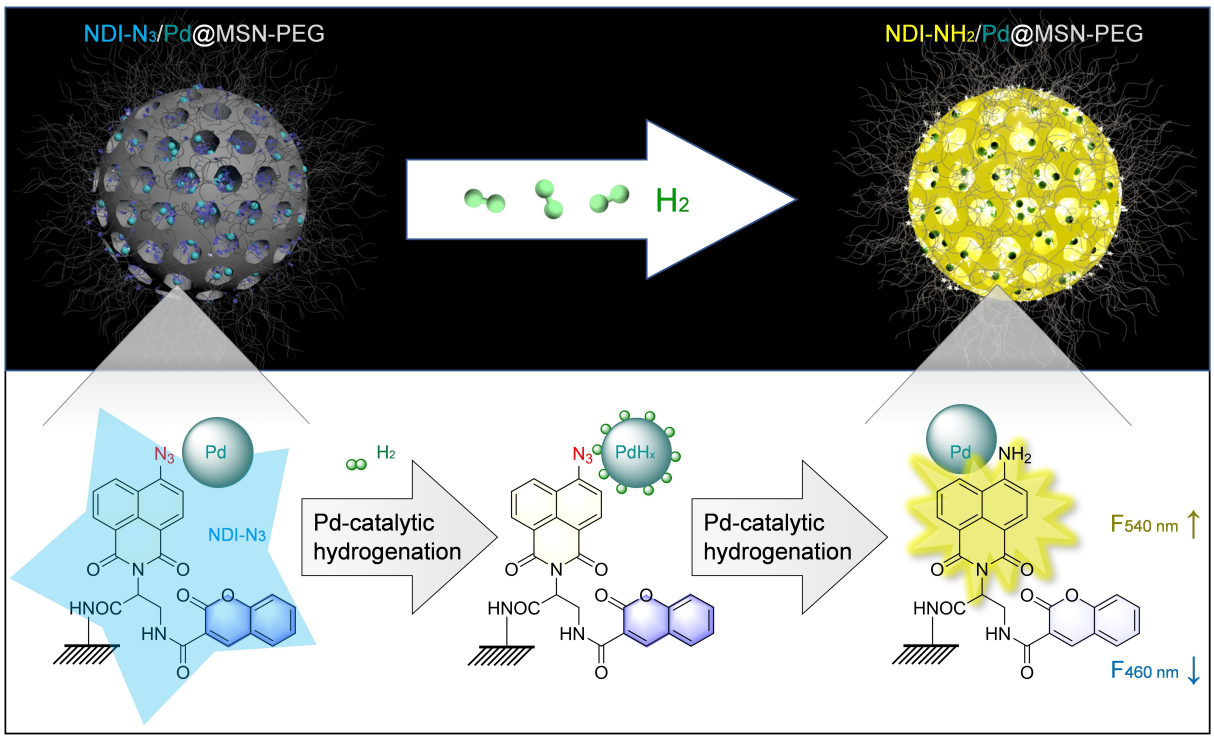

Figure 1. Illustration of the structure and detection mechanism of the ratiometric fluorescent hydrogen probe of NDI-N_3/Pd@MSN-PEG.

sharp fluorescence enhancement within 20 s after H_2 bubbling (Route (3), Figure S1c,d).

Next, we used MSN to encapsulate both the catalytic segment Pd nanoparticles and the detection segment within plentiful mesoporous channels to improve the aqueous dispersion of the whole system and to enhance the detection sensitivity of single particles. Within the mesoporous channels of MSN, NDI′-N_3-TPY was directly attached onto Pd nanoparticles through coordination attraction (as illustrated by Route (4) in Figure S2), but catalytic hydrogenation efficiency was relatively low (Figure S2a), possibly because of NDI′-N_3-TPY aggregation-induced fluorescence quenching and/or high steric hinderance for intramolecular folding. To overcome this issue, we covalently fixed the detection segment onto the mesopore channel surface of MSN to increase its loading capacity for enhanced contact with Pd nanoparticles and also to avoid its fluorescence quenching (Route (5) in Figure S2). The catalytic hydrogen efficiency and sensitivity became considerably high, indicating high feasibility of the molecular fixing route (Figure S2b). Furthermore, we supplemented coumarin as a fluorescence reference to construct the ratiometric probe (Route (6) in Figure S3).

Probe synthesis and characterization

Based on the above-proposed Route (6), NDI-N_3 was firstly synthesized and then conjugated onto Pd@MSN to construct the NDI-N_3/Pd@MSN-PEG probe. The NDI-N_3 synthesis route is demonstrated in Figure 2a. Naphthalic anhydride was chose as detection fluorophore because of its high photostability and high resistance to chemical reactions. First, the bromine on NDO-Br was replaced with N_3 and then NDO-N_3 was linked with a coumarin derivate Cou-NH_2 to obtain NDI-N_3 (Figure 2a). The structures of various intermediates and the final product NDI-N_3 were confirmed by NMR and MS characterization (Figure 2b; Figures S4–S7). The synthesized NDI-N_3 exhibited characteristic fluorescence profiles of coumarin and naphthalimide, with distinct blue and green fluorescence emissions at 460 nm (375 nm excitation) and 540 nm (435 nm excitation; Figure S8) for which the intensities were significantly enhanced after reaction with hydrogen molecules in the aqueous solution of Pd nanoparticles (Figure 2c), owing to Pd-catalyzed hydrogenation/reduction of azide into amine. The ratio between fluorescence intensities at 542 nm and 460 nm (420 nm excitation) rapidly increased from 1.7 to 39.1 after 120 s catalytic hydrogenation (Figure 2c).

Pd@MSN was synthesized by a typical induction growth method (Figure 2d).[26] First, MSN was prepared by a template method and then modified with amino groups by a silane coupling method, which induces in situ growth of Pd nanoparticles within the mesoporous channels of MSN and allows further NDI-N_3 conjugation and PEG modification in favor of water dispersion improvement (Figure 2d). From STEM images in Figure S9, the as-synthesized MSN displayed a uniform particle size of about 100 nm and a clear porous structure with an average pore size of about 5 nm, in agreement with prior literature,[26] which was not affected by subsequent amino modification (Figure S10), Pd deposition (Figure S11), NDI-N_3 conjugation (Figure S12), and PEG modification (Figure S13). The finally obtained NDI-N_3/Pd@MSN-PEG probe showed good dispersion in aqueous solution and a narrow size distribution with an average hydrated diameter of 120 nm (Figure S14). HADDF image and elementary mapping results (Figure 2e,f) clearly indicated that large amounts of Pd nanoparticles were dispersed within the mesoporous channels. The Pd size was statistically measured to be about 1–2 nm from the HADDF images, in accord with the literature.[26] There is enough pore space for molecular diffusion in the pore channels of Pd@MSN, in support of NDI-N_3 modification. The Pd and NDI-N_3 loading capacities of NDI-N_3/Pd@MSN-PEG were measured to be 19.7 mg g^{-1} and 2.6 mg g^{-1} by inductively coupled plasma emission spectrometry and elemental analysis, respectively. The mesoporous channels of MSN prevented Pd nanoparticles from aggregation and over-growth, which is helpful to the efficiency of the catalyst, and the high surface area of MSN provided a plentiful internal surface for a high NDI-N_3/Pd payload in support of high detection sensitivity.

Hydrogen molecular detection behaviors

The performances of the above-developed hydrogen molecular probe NDI-N_3/Pd@MSN-PEG involving sensitivity, selectivity, and detection limit were investigated. First, hydrogen gas was continuously bubbled into the aqueous solution containing the probe to ensure a plentiful and constant amount of hydrogen molecules for detection. The fluorescence intensity at 542 nm quickly increased with time (Figure 3a,b), while that at 460 nm decreased to a certain extent, possibly because fluorescence resonance energy transfer (FRET) from coumarin to naphthalimide caused a decrease in the fluorescence intensity of coumarin. More importantly, the ratio between fluorescence intensities at 542 and 460 nm also increased quickly (Figure 3b), suggesting considerable sensitivity of the probe. On the other hand, the NDI-N_3/Pd@MSN-PEG probe was dispersed into different concentrations of H_2-containing water to react for the same period of time (30 min, Figure 3c). The ratio of green to blue fluorescence intensity increased almost linearly when the molecular concentration of hydrogen went up to 800 μM (Figure 3d). In addition to the green/blue (G/B) fluorescence ratio, the green fluorescence increase rate ($\Delta I/I_0$ @ 542 nm) was also used to monitor the molecular concentration of hydrogen (Figure 3e). Furthermore, the hydrogen detection limit of the probe was measured to be 26.7 nM by the classic method when a sufficient amount of probe was used (Figure S15).

Besides low detection limit and real-time tracing ability, rapid detection is also of vital importance to the sensitivity of hydrogen detection because of its high diffusibility. The reaction dynamic process of the probe reacting with saturated H_2-rich water (HRW, 0.8 mM) was observed. The green fluorescence increase rate ($\Delta I/I_0$ @ 542 nm) exhibited

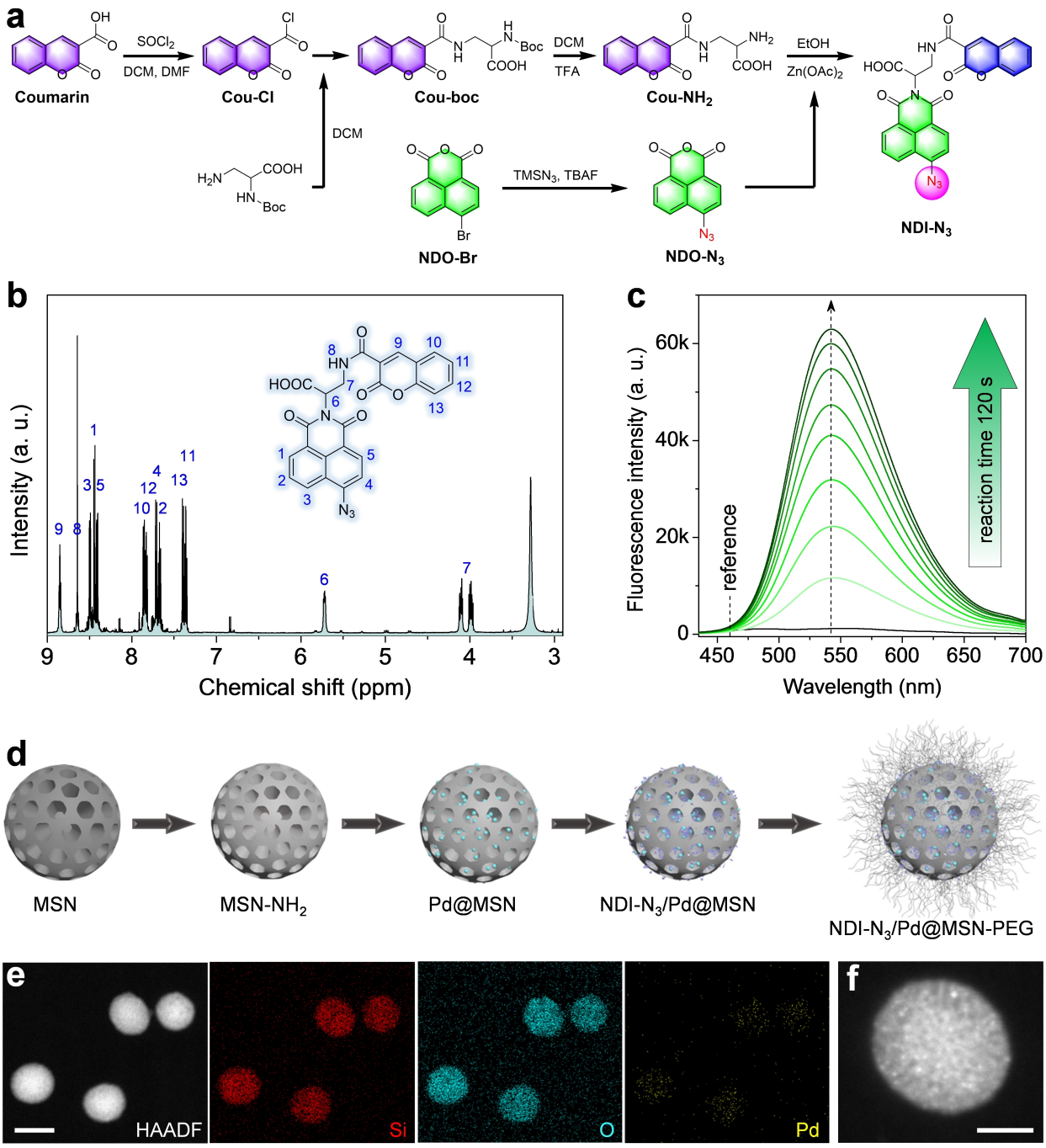

Figure 2. Synthesis and characterization of the hydrogen probe. a) Synthesis route of NDI-N_3. b) ^{1}H NMR spectrum of NDI-N_3. c) Fluorescence spectra of NDI-N_3 before and after reaction with H_2 catalyzed by Pd nanoparticles. d) Synthesis route of the NDI-N_3/Pd@MSN-PEG probe. e) HADDF image and corresponding elementary mapping of NDI-N_3/Pd@MSN-PEG, and f) High-resolution HADDF image of NDI-N_3/Pd@MSN-PEG. Scale bars in (e) and (f) correspond to 100 and 50 nm, respectively.

a linear relationship with reaction time, indicating that the reaction rate was constant and quick so that the detection reaction cannot be restricted by molecular diffusion (Figure 3f). It took about 6 min for the detection reaction to achieve a balance, indicating that the as-prepared hydrogen probe was able to complete the catalytic hydrogenation reaction in a relatively short time. Such a response speed is comparable to that of conventional gas chromatography and many general molecular probes, ensuring the synthesized hydrogen probe is applicable for hydrogen detection in living organisms.

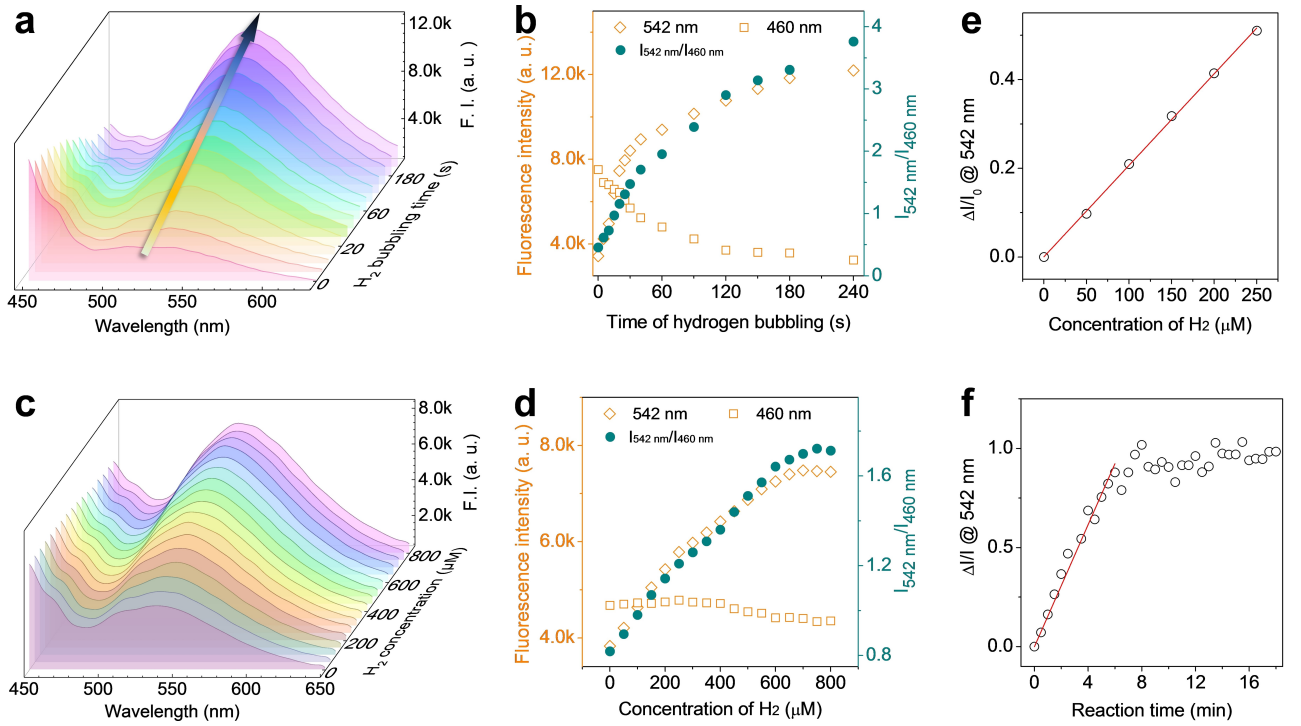

Figure 3. Hydrogen detection performances in solution. a) Fluorescence spectra of the aqueous solution of the NDI-N_3/Pd@MSN-PEG probe during hydrogen gas bubbling. b) The corresponding statistical plot of (a). c) Fluorescence spectra of the hydrogen-containing aqueous solution of the probe after reaction for 30 min. d,e) The corresponding statistical plot of (c). f) The reaction rate of the probe in saturated HRW.

Intracellular hydrogen detection performance

Based on the ideal performances of the probe in the aqueous solution, we further investigated its hydrogen detection performances in cells where biomembranes need to be crossed. Firstly, a simple probe NDI″-N_3/Pd@MSN-PEG (Figure S2) was used to explore the feasibility of intracellular hydrogen detection. From Figure S16, the NDI″-N_3/Pd@MSN-PEG probe can quickly image intracellular hydrogen molecules as its green fluorescence remarkably increased in response to the addition of H_2-rich PBS (HRPBS) on a confocal laser scanning microscope (CLSM). Furthermore, the ratiometric fluorescent probe NDI-N_3/Pd@MSN-PEG was used to enhance the accuracy of intracellular hydrogen detection. The NDI-N_3/Pd@MSN-PEG probe was firstly incubated with B16 cells for 3 h for cellular uptake, and residual nanoparticles outside cells were washed off with PBS, followed by the addition of HRPBS and immediate fluorescence observation on the CLSM. It was clearly visible that intracellular green fluorescence instantly increased after HRPBS was added (Figure 4a). The statistical data further indicated that, in the absence of hydrogen water, the G/B ratio (fluorescence intensity ratio between green and blue channels) was basically maintained at about 0.56 (Figure 4b), whereas after the addition of HRPBS the G/B value increased rapidly by 12 % in 0.5 min, and to 1.98 times in 1.5 min, and then kept almost steady (Figure 4b). These results demonstrated that the developed hydrogen probe could indeed detect hydrogen molecules in the cellular environment, and its short response time not only proved that our developed hydrogen probe had the ability to detect hydrogen molecules in cells in real time, but also directly confirmed that hydrogen molecules were able to easily cross the cellular membrane for quick transmembrane transport in seconds.

Furthermore, the selectivity and stability of the NDI-N_3/Pd@MSN-PEG probe were investigated since the physiological environment is complicated. Several kinds of common anions and cations in the physiological environment, including Na^+, Ca^{2+}, Mg^{2+}, Cl^-, $H_2PO_4^-$, etc., were investigated. The G/B ratio of the probe was not affected at the physiological concentrations (Figure 4d; Figure S17) or at the uniform super-high concentration (500 mM, Figure S17) of these ions, indicating high selectivity of the probe. Moreover, the selectivity of the probe to typical reductive substances in the body, including reductive glutathione (GSH), ascorbic acid (AA), cysteine (Cys), and $NaHSO_3$ was further investigated since the detection mechanism of the probe was based on chemical reduction. GSH, Cys, and $NaHSO_3$ slowly caused a slight increase in fluorescence intensity, but the magnitude and speed of changes were far lower than that of the same concentration of hydrogen molecules (0.8 mM, Figure 4e), possibly because these reductive substances cannot be catalyzed by Pd for hydrogenation, but they directly reduced azide in the probe in relatively low efficiency. In addition, the intracellular stability of the probe was investigated by co-incubation with cells for an extended period of time. The G/B ratio of probe-treated cells was maintained around 0.6 within 24 h, and the probe did not exhibit obvious cytotoxicity (Fig-

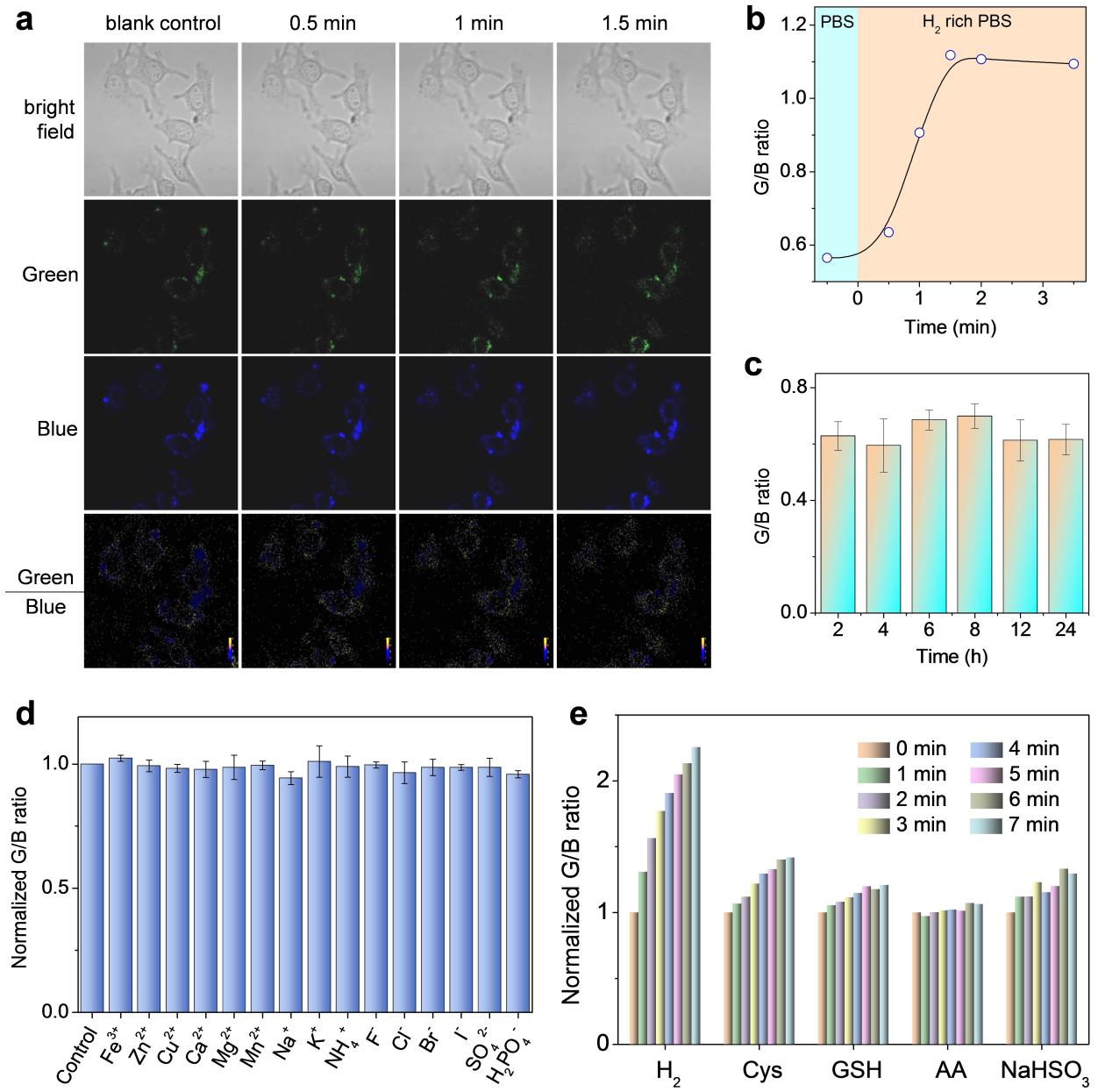

Figure 4. Hydrogen detection performances in cells. a) Fluorescence images of probe-treated cells before and after HRPBS incubation. b) The corresponding G/B ratio. c) The G/B ratio of B16 cells treated with the probe for different time durations. d) The normalized G/B ratio of various ionic solutions treated with the probe. e) The normalized G/B ratio of various solutions of reductants treated with the probe for different time durations.

ure 4c; Figure S18). This suggested that the probe was stable enough in the cellular environment, enabling long-term and stable detection of intracellular hydrogen molecules.

In vivo hydrogen detection performances

In vivo hydrogen detection performances of the developed probe were further investigated using two representative models of animals and plants to check the feasibility of in vivo hydrogen detection and also to directly confirm the in vivo transmembrane ability of hydrogen molecules. The BBB as one of the biological barriers that is challenging to overcome was chosen for investigation. As demonstrated in Figure 5a, mouse skull was removed under anesthesia and then the PBS solution of NDI-N_3/Pd@MSN-PEG probe was dropped on the surface of the left brain for imaging, while the right side was retained as a blank control. After H_2 inhalation for 5 min at a speed of 300 mL min^{-1}, the mouse brain was immediately fluorescence-imaged at two emission channels of 500 nm (excitation wavelength, 430 nm) and 540 nm (excitation wavelength, 465 nm), and then the inhalation gas was switched to air. After air inhalation for 4 min, the mouse brain was immediately fluorescence-

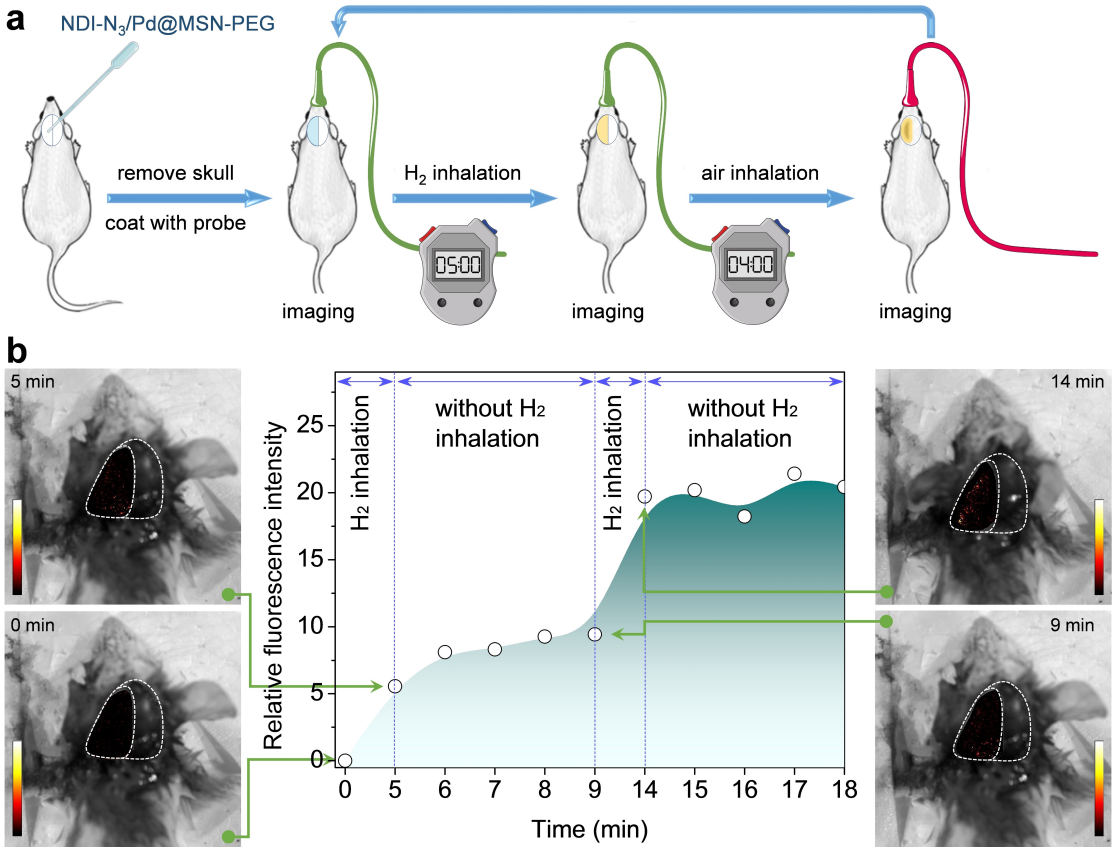

Figure 5. a) Illustration of hydrogen detection using the probe in the mouse model. b) Relative fluorescence intensity of the brain and corresponding fluorescence images at several representative time points.

imaged again. The same procedure of H_2-to-air inhalation and fluorescence imaging was repeated once. ImageJ software was used to process the original fluorescence images (Figures S19–S21) by a standard method (see the Methods section in the Supporting Information), and the relative fluorescence intensity in Figure 5b and Figure 6b reflect the G/B ratio.

Analysis of the results revealed that 5 min of hydrogen inhalation caused significant enhancement of fluorescence intensity in the treated brain, indicating that hydrogen molecules rapidly crossed the BBB and reacted with the probe (Figure 5b). In addition, the midway 4 min of air inhalation did not lead to visible fluorescence enhancement, owing to no supply of hydrogen molecules. Another 5 min of hydrogen inhalation resulted in fluorescence enhancement again, which could be immediately terminated by subsequent air inhalation. This suggested that the probe had both high responsivity and high sensitivity for in vivo hydrogen detection. Another mouse was used to repeat this experiment, and the same detection results were obtained (Figure S20), confirming the reliability of the present results. It is worth noting that this is the first direct evidence of hydrogen molecules crossing the BBB, which explains why hydrogen inhalation can effectively treat neurodegenerative diseases, as concluded by many clinical reports.[27–31] In addition, the presented results imply that continuous and long-term supply of hydrogen molecules is necessary to maintain high hydrogen dosage in the brain for efficient treatment of these diseases,[4] possibly owing to high dispersion and low solubility of hydrogen molecules.

We next investigated the transport of hydrogen molecules from root to leaf (15 cm in distance) in a plant model of *Ageratum conyzoides L.* since hydrogen molecules are involved in controlling some important physiological processes in plants, such as drought resistance. The aqueous solution of the NDI-N_3/Pd@MSN-PEG probe was dropped on the surface of leaves and became dried naturally, and then its root was put into ionized water (10 mL) in a tube for fluorescence imaging as a blank control (Figure 6a). Water was replaced with freshly prepared saturated HRW, and then leaves were immediately fluorescence-imaged at two emission channels of 500 nm (excitation wavelength, 430 nm) and 540 nm (excitation wavelength, 465 nm). After immersion for 5 min, HRW was refreshed and the leaves were fluorescence-imaged again. As shown in Figure 6b, when the plant root was immersed in saturated HRW, fluorescence of the leaves rapidly enhanced in seconds, reached the maximum within 2 min and then was unchanged, indicating that hydrogen molecules were rapidly absorbed by the root and transported along the stem to the leaves. Intriguingly, hydrogen molecules that can so easily cross the biological barriers of plants and exhibit a high transport speed, have not been reported previously. Moreover, another fluorescence enhancement after refreshing the

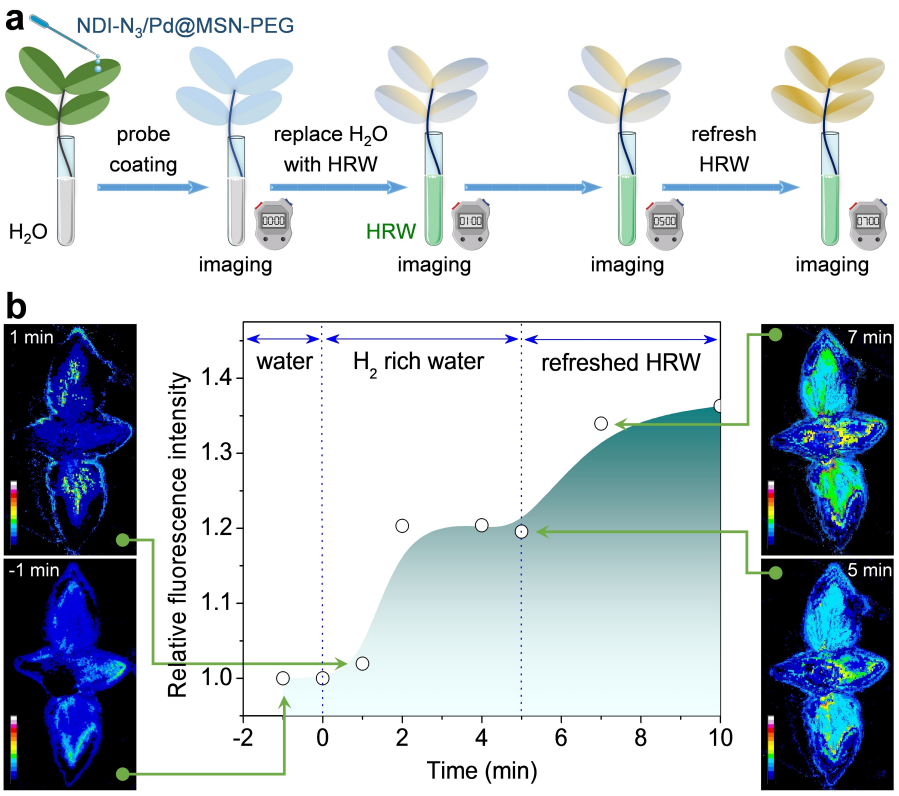

Figure 6. a) Illustration of hydrogen detection using the probe in the plant model. b) Relative fluorescence intensity of the leaves and corresponding fluorescence images at several representative time points.

HRW was attributed to quick escape of hydrogen molecules from HRW; this suggests that a sustained supply of hydrogen molecules might be necessary for hydrogen agriculture.[32]

Conclusion

In summary, to address the issue of hydrogen detection in living organisms, we developed a ratiometric fluorescent probe based on a catalytic hydrogenation strategy, which consisted of Pd nanoparticles as a hydrogenating catalyst, azide-modified fluorophore responsible for the fluorescence response to catalytic hydrogenation, and MSN as a carrier. The probe was able to rapidly react with hydrogen molecules under mild conditions for responsive fluorescence. Based on the rapid response of the probe to hydrogen molecules, we directly confirmed the super-fast diffusion and ultrahigh transmembrane transport properties of hydrogen molecules at the cellular, animal, and plant levels. The present results will provide help and inspiration for recognition and understanding of the underlying biological behaviors and mechanisms of hydrogen molecules.

Acknowledgements

We greatly appreciate discussions with Prof. Xuejun Sun (SJTU, SMMU), and the Instrumental Analysis Center of Shenzhen University (XiLi campus) for assistance in material characterization. Funding: this work was supported by the National Natural Science Foundation of China (51872188 and 82172078), Shenzhen Basic Research Program (SGDX20201103093600004), Special Funds for the Development of Strategic Emerging Industries in Shenzhen (20180309154519685), SZU Top Ranking Project (860-00000210), the Academic Promotion Project of Shandong First Medical University (2019ql010 and 2019pt009), and Center of Hydrogen Science, Shanghai Jiao Tong University, China.

Conflict of Interest

The authors declare no conflict of interest.

Data Availability Statement

The data that support the findings of this study are available in the Supporting Information of this article.

Keywords: Fluorescence imaging · Hydrogen medicine · Mesoporous silica nanoparticles · Molecular imaging probe

[1] M. Dole, F. Wilson, W. Fife, *Science* **1975**, *190*, 152.
[2] I. Ohsawa, M. Ishikawa, K. Takahashi, M. Watanabe, K. Nishimaki, K. Yamagata, K. Katsura, Y. Katayama, S. Asoh, S. Ohta, *Nat. Med.* **2007**, *13*, 688.
[3] J. Li, C. Wang, J. H. Zhang, J. M. Cai, Y. P. Cao, X. J. Sun, *Brain Res.* **2010**, *1328*, 152.
[4] L. Zhang, P. Zhao, C. Yue, Z. Jin, Q. Liu, X. Du, Q. He, *Biomaterials* **2019**, *197*, 393.
[5] Z. Jin, Y. Sun, T. Yang, L. Tan, P. Lv, Q. Xu, G. Tao, S. Qin, X. Lu, Q. He, *Biomaterials* **2021**, *276*, 121030.
[6] P. Zhao, Z. Jin, Q. Chen, T. Yang, D. Chen, J. Meng, X. Lu, Z. Gu, Q. He, *Nat. Commun.* **2018**, *9*, 4241.
[7] B. Zhao, Y. Wang, X. Yao, D. Chen, M. Fan, Z. Jin, Q. He, *Nat. Commun.* **2021**, *12*, 1345.
[8] W. L. Wan, Y. J. Lin, H. L. Chen, C. C. Huang, P. C. Shih, Y. R. Bow, W. T. Chia, H. W. Sung, *J. Am. Chem. Soc.* **2017**, *139*, 12923.
[9] J. Zeng, Z. Ye, X. Sun, *Med. Gas Res.* **2014**, *4*, 15.
[10] Z. Dong, L. Wu, B. Kettlewell, C. D. Caldwell, D. B. Layzell, *Plant Cell Environ.* **2003**, *26*, 1875.
[11] C. Li, T. Gong, B. Bian, W. Liao, *Funct. Plant Biol.* **2018**, *45*, 783.
[12] M. Wu, X. Xie, Z. Wang, J. Zhang, Z. Luo, W. Shen, J. Yang, *Plant Physiol. Biochem.* **2021**, *163*, 317.
[13] Q. Jin, K. Zhu, W. Cui, L. Li, W. Shen, *J. Plant Growth Regul.* **2016**, *35*, 565.
[14] C. Liu, R. Kurokawa, M. Fujino, S. Hirano, B. Sato, X.-K. Li, *Sci. Rep.* **2014**, *4*, 5485.
[15] R. Yamamoto, K. Homma, S. Suzuki, M. Sano, J. Sasaki, *Sci. Rep.* **2019**, *9*, 1255.
[16] K. J. Bruemmer, S. W. M. Crossley, C. J. Chang, *Angew. Chem. Int. Ed.* **2020**, *59*, 13734; *Angew. Chem.* **2020**, *132*, 13838.
[17] D. A. Iovan, S. Jia, C. J. Chang, *Inorg. Chem.* **2019**, *58*, 13546.
[18] J. Chan, S. C. Dodani, C. J. Chang, *Nat. Chem.* **2012**, *4*, 973.
[19] Q. Yang, Y.-Z. Chen, Z. U. Wang, Q. Xu, H.-L. Jiang, *Chem. Commun.* **2015**, *51*, 10419.
[20] Y. Wang, Y. Deng, F. Shi, *J. Mol. Catal. Chem.* **2014**, *395*, 195.
[21] M. A. Mahdaly, J. S. Zhu, V. Nguyen, Y.-S. Shon, *ACS Omega* **2019**, *4*, 20819.
[22] N. Arai, N. Onodera, T. Ohkuma, *Tetrahedron Lett.* **2016**, *57*, 4183.
[23] A. R. Lippert, E. J. New, C. J. Chang, *J. Am. Chem. Soc.* **2011**, *133*, 10078.
[24] V. S. Lin, A. R. Lippert, C. J. Chang, *Proc. Natl. Acad. Sci. USA* **2013**, *110*, 7131.
[25] V. S. Lin, W. Chen, M. Xian, C. J. Chang, *Chem. Soc. Rev.* **2015**, *44*, 4596.
[26] D. Shen, L. Chen, J. Yang, R. Zhang, Y. Wei, X. Li, W. Li, Z. Sun, H. Zhu, A. M. Abdullah, A. Al-Enizi, A. A. Elzatahry, F. Zhang, D. Zhao, *ACS Appl. Mater. Interfaces* **2015**, *7*, 17450.
[27] K. Nishimaki, T. Asada, I. Ohsawa, E. Nakajima, C. Ikejima, T. Yokota, S. Ohta, *Curr. Alzheimer Res.* **2018**, *15*, 482.
[28] C. T. Hong, C. J. Hu, H. Y. Lin, D. Wu, *Medicine* **2021**, *100*, e24191.
[29] H. Ono, Y. Nishijima, S. Ohta, M. Sakamoto, K. Kinone, T. Horikosi, M. Tamaki, H. Takeshita, T. Futatuki, W. Ohishi, T. Ishiguro, S. Okamoto, S. Ishii, H. Takanami, *J. Stroke. Cerebrovasc. Dis.* **2017**, *26*, 2587.
[30] A. Yoritaka, T. Abe, C. Ohtsuka, T. Maeda, M. Hirayama, H. Watanabe, H. Saiki, G. Oyama, J. Fukae, Y. Shimo, T. Hatano, S. Kawajiri, Y. Okuma, Y. Machida, H. Miwa, C. Suzuki, A. Kazama, M. Tomiyama, T. Kihara, M. Hirasawa, H. Shimura, N. Hattori, *BMC Neurol.* **2016**, *16*, 66.
[31] A. Yoritaka, M. Takanashi, M. Hirayama, T. Nakahara, S. Ohta, N. Hattori, *Mov. Disord.* **2013**, *28*, 836.
[32] Y. Wang, P. Lv, L. Kong, Q. He, W. Shen, *Chem. Eng. J.* **2021**, *405*, 126905.
[33] Y. Xie, Y. Mao, W. Zhang, D. Lai, Q. Wang, W. Shen, *Plant Physiol.* **2014**, *165*, 759.

Manuscript received: October 27, 2021
Accepted manuscript online: December 17, 2021
Version of record online: ■■, ■■

Research Articles

Fluorescent Probes

W. Gong, L. Jiang, Y. Zhu, M. Jiang,
D. Chen, Z. Jin, S. Qin, Z. Yu,*
Q. He* _____ **e202114594**

An Activity-Based Ratiometric Fluorescent Probe for In Vivo Real-Time Imaging of Hydrogen Molecules

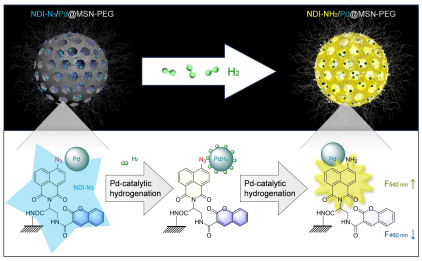

A ratiometric fluorescent hydrogen probe was developed for the first time by a catalytic hydrogenation strategy, enabling efficient detection of hydrogen molecules in vivo and in vitro with high sensitivity, rapid responsivity, high selectivity and low detection limit, in favor of uncovering and understanding underlying biological behaviors and mechanisms of hydrogen molecules.